

This is an electronic reprint of the original article. This reprint may differ from the original in pagination and typographic detail.

---

## Reaction engineering approach to the synthesis of sodium borohydride

Salmi, Tapio; Russo, Vincezo

*Published in:*  
Chemical Engineering Science

*DOI:*  
[10.1016/j.ces.2019.01.007](https://doi.org/10.1016/j.ces.2019.01.007)

Publicerad: 01/01/2019

*Document Version*  
(Referentgranskad version om publikationen är vetenskaplig)

*Document License*  
CC BY-NC-ND

[Link to publication](#)

*Please cite the original version:*  
Salmi, T., & Russo, V. (2019). Reaction engineering approach to the synthesis of sodium borohydride. *Chemical Engineering Science*, 199, 79–87. <https://doi.org/10.1016/j.ces.2019.01.007>

### General rights

Copyright and moral rights for the publications made accessible in the public portal are retained by the authors and/or other copyright owners and it is a condition of accessing publications that users recognise and abide by the legal requirements associated with these rights.

### Take down policy

If you believe that this document breaches copyright please contact us providing details, and we will remove access to the work immediately and investigate your claim.

# Reaction engineering approach to the synthesis of sodium borohydride

Tapio Salmi\*, Vincenzo Russo

Åbo Akademi, PCC/Chemical Engineering, Laboratory of Industrial Chemistry and Reaction Engineering, FI-20500 Turku/Åbo, Finland

Università di Napoli 'Federico II', Chemical Sciences Department, IT-80126 Napoli, Italy

\* Corresponding author: [tapio.salmi@abo.fi](mailto:tapio.salmi@abo.fi), tel. +358 2 2154427, fax. +358 2 2154479

## ABSTRACT

A mathematical model for the synthesis of sodium borohydride ( $\text{NaBH}_4$ ) from finely dispersed solid sodium hydride ( $\text{NaH}$ ) and dissolved trimethyl borate ( $\text{B}(\text{OH})_3$ ) in inert mineral oil was developed. The model is based on a plausible reaction mechanism of dissolved and adsorbed trimethyl borate on the surface of sodium hydride, where the reaction is presumed to take place. The surface reaction between sodium hydride and trimethyl borate leads to the formation of main ( $\text{NaBH}_4$ ) and side products (methoxy borohydrides), which was verified by chemical analysis of sodium borohydride and methanol in the water extract of the oil phase. Extensive kinetic experiments in a laboratory-scale isothermal and isobaric slurry reactor enabled a detailed kinetic analysis of the data, including the derivation of a mathematical model for the formation of sodium borohydride in a semibatch slurry reactor. The kinetic model was verified with experimental information and can be used as an element for process design.

Keywords: sodium borohydride, trimethyl borate, synthesis, kinetics, slurry reactor, mathematical model

## 1 INTRODUCTION

Sodium borohydride (tetrahydroborate,  $\text{NaBH}_4$ ) is a very exciting chemical component. Four hydride groups are attached to a single sodium atom, which gives a strong but very selective reducing power to the compound [1-2]. Sodium borohydride was discovered in 1940's in the USA by H.J. Schlesinger and H.C. Brown. Because of the strategic and military importance of the hydroboron compounds, the pioneering work was published much later, in 1953 [3-5]. H.C. Brown obtained the Nobel Prize in chemistry in 1979 for his breakthrough research in organic boron compounds.

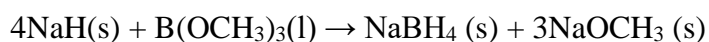
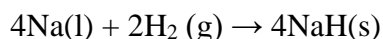
The industrial use of  $\text{NaBH}_4$  is widespread, such as in the production of bleaching agents, fine chemicals and pharmaceuticals, and in the reduction of metals for catalyst manufacturing. Sodium borohydride is a very selective reducing agent of organic compounds, converting ketones and aldehydes to alcohols, but saving other functional groups. It is able to reduce acyl chlorides, thiol esters and imines and it is used in the synthesis of vitamin A. Sodium borohydride is consumed in huge amounts in the production of the common bleaching agent for pulp and dying industries, sodium dithionite from sulphur dioxide. Because of its special molecular structure, and high hydrogen content,  $\text{NaBH}_4$  is a potential hydrogen storage component in fuel cells. Even though more environmentally friendly ways for reduction, such as the use of molecular hydrogen are continuously investigated,  $\text{NaBH}_4$  has preserved its position as one of the important reagents in modern chemical industry [1-2].

Sodium borohydride is commercially available both in solid form and as alkaline solutions. In an alkaline milieu, at  $\text{pH}=14$ ,  $\text{NaBH}_4$  is kinetically very stable and can be safely stored long times. Under acidic conditions  $\text{NaBH}_4$  reacts vigorously with water releasing hydrogen. Thus the safety aspects are very important in the storage and use of  $\text{NaBH}_4$ . The decomposition of  $\text{NaBH}_4$  can be predicted at various  $\text{pH}$ -values and temperatures by a kinetic model published in ref. [6]. The kinetic stability at high  $\text{pH}$  along with the selective reductive power of  $\text{NaBH}_4$  is the main reason for its usefulness and success in the synthetic chemical industry.

Several routes for the large-scale synthesis of  $\text{NaBH}_4$  have been investigated, such as the Borax process of Bayer AG [7], the tetrafluoroborate process developed at the Czechoslovak Academy

Sciences [8], multistep thermal reductions [9], and metallic reduction agents [9]. Attempts have also been made to replace sodium with the less expensive magnesium in the Borax process [10]. The potential of various process alternatives are reviewed by Wu et al [9], who conclude that many of the proposed processes contain either thermodynamically unfavourable steps or require many process steps. They predict that electrochemical production processes could be developed to make sodium borohydride in a less expensive way.

However, the process concept proposed by Schlesinger and Brown [3-5] is still the dominant one. It is based on the direct reaction of dissolved trimethyl borate ( $B(OCH_3)_3$ ) with finely dispersed sodium hydride (NaH) in an inert mineral oil at 250-270°C. This process step is a logical continuation of the previous step, i.e. the production of solid NaH by hydrogenation of liquid sodium by molecular hydrogen in a mineral oil dispersion. In the first process step, a complete conversion of sodium to NaH can be achieved and the dispersion of NaH is taken to the next process step, synthesis of  $NaBH_4$  [1-2]. Both process steps require an intensive agitation to keep sodium as small droplets in the dispersion and to transfer molecular hydrogen and  $B(OH)_3$  to the reaction mixture. Continuous operation is possible by coupling tank reactors in series. The overall reactions in the production of  $NaBH_4$  are listed below,



By extracting the product dispersion with water,  $NaBH_4$  is dissolved in the aqueous phase and  $NaOCH_3$  forms  $NaOH$  and  $CH_3OH$  in the aqueous phase. The mineral oil is recycled – in fact it is the working solution of the process.  $CH_3OH$  is evaporated from the aqueous phase and is brought in contact with boric acid ( $B(OH)_3$ ) to obtain  $B(OCH_3)_3$ . A concentrated, strongly alkaline  $NaBH_4$  solution is obtained from the water extraction step. This solution can be used as such, for example, in the production of the bleaching agent sodium dithionite, or dissolved  $NaBH_4$  can be extracted with an amine and crystallized to obtain pure, solid  $NaBH_4$ . The process is complicated and very demanding from chemical, technical and safety viewpoints.

In spite of the long history – more than 70 years – of the synthesis of  $NaBH_4$ , most of the previous publications (see e.g. [1-2]) devoted to the topic are of qualitative character, reporting

the reactant conversion and product selectivity after a fixed synthesis time but not treating the rate of the reaction, the quantitative kinetic aspects. In the present article, systematic kinetic data on the synthesis of  $\text{NaBH}_4$  from  $\text{NaH}$  and  $\text{B}(\text{OH})_3$  will be presented and discussed, followed by an advancing modelling effort of the multiphase system. The endeavour of the current work is to provide a comprehensive view on the synthesis kinetics of  $\text{NaBH}_4$  under industrially relevant conditions.

## **2 STOICHIOMETRY, MECHANISM, KINETICS AND REACTOR MODEL**

### **2.1 Model hypotheses**

Some fundamental hypotheses were made before deriving the mathematical model for the formation of sodium borohydride from sodium hydride and trimethyl borate. The reaction is presumed to progress stepwise in an inert mineral oil so that the boron atom in dissolved trimethyl borate gets a hydride substituent from solid  $\text{NaH}$  in successive steps. The methoxy groups leave stepwise the trimethyl borate forming sodium methoxide. The final product is dispersed solid  $\text{NaBH}_4$  in mineral oil. The reaction steps are assumed to be irreversible. The reaction could principally proceed as a reaction between adsorbed trimethyl borate and  $\text{NaH}$  on the solid surface, or as a reaction between trimethyl borate from liquid and the  $\text{NaH}$  surface. However, taking into consideration the stepwise character of the process, i.e. the successive replacement of methoxy groups by hydride in trimethyl borate, the adsorption hypothesis of trimethyl borate is more plausible.

Based on the above reasoning, the reaction assumed to proceed at the outer surface of the very small sodium hydride particles ( $d_p=10\text{-}15\mu\text{m}$ ) and the reaction products leave the sodium hydride surface, thus no product layer is formed. This hypothesis requires vigorous stirring of the dispersion. Because of vigorous stirring, the mass transfer resistance of trimethyl borate is negligible around the sodium hydride particles. For the sake of simplicity, the  $\text{NaH}$  particles are presumed to have equal sizes in the beginning of the reaction. Trimethyl borate is continuously fed to the system during the process and the change of the liquid volume due to the addition of trimethyl borate is included in the mathematical model. The other components ( $\text{NaH}$ ,  $\text{NaOCH}_3$ ,

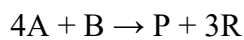
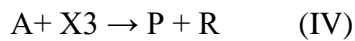
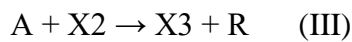
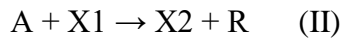
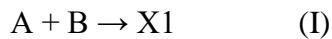
methoxyborohydrides, NaBH<sub>4</sub>) are in batch. The semibatch reactor operates under isothermal and isobaric conditions.

## 2.2 Reaction stoichiometry

Based on the hypotheses presented in the previous section, the successive reaction steps can be written as



As revealed by the stoichiometric scheme, the reaction system is a parallel system with respect to NaH (A), but a consecutive system with respect to B(OCH<sub>3</sub>)<sub>3</sub> (B). The reaction mechanism can be expressed in a compressed form,

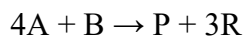
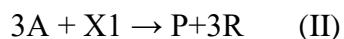
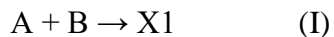


## 2.3 Reaction mechanism and rate equations

The complete competitive-consecutive reaction stoichiometry displayed in steps I-IV above. Based on this mechanism, simulations of the product distribution can be conducted, provided that the numerical values of the rate constants are available.

Sodium trimethoxy borohydride (X1) (melting point 230°C) is the only intermediate, which has been confirmed experimentally [3-5]. The evidence of the other intermediates (X2 and X3) has not been confirmed directly, but they follow a logical chemical reasoning: the boron atom receives new hydride step-by-step, until solid sodium borohydride (P) (melting point 505°C) is finally formed. Sodium methoxide (R) is released in each step, because a methoxy group in trimethyl borate is replaced by a hydride group.

Based on the fact that X1 is observed experimentally, but X2 and X3 not, it is reasonable to presume that reaction steps I and II are slow, whereas the subsequent steps III-IV can be merged to a pseudo-step. The simplified mechanism is obtained,



The simplified vector for the components becomes  $\mathbf{a}'^T = [A \ B \ X1 \ P \ R]$  and the stoichiometric matrix is written as

$$N' = \begin{bmatrix} -1 & -3 \\ -1 & 0 \\ +1 & -1 \\ 0 & +1 \\ 0 & +3 \end{bmatrix} \quad (1)$$

The generation rates are obtained from

$$\mathbf{r} = N'\mathbf{R}' \quad (2)$$

By assuming that the first hydride addition in step II is rate-determining, the kinetics of steps I-II can be expressed as

$$R_1' = k_1 c_A^* c_B^* \quad (3)$$

$$R_2' = k_2 c_A^* c_{X1}^* \quad (4)$$

In this kind of fluid-solid reactions, the surface concentration of A is assumed to be constant, because it reflects the total amount of NaH per surface unit. The effect of NaH is taken into account in the mass balance for the reactor, where it is assumed that the total consumption or production is proportional to the available area of solid (see Section 2.4). This reasoning implies that the rate equations for steps I and II can be expressed by

$$R_1' = k_1' c_B^* \quad (5)$$

$$R_2' = k_2' c_{X1}^* \quad (6)$$

where the lumped constants are  $k_1' = k_1 c_A^*$  and  $k_2' = k_2 c_A^*$ . The concentrations of B and X1 on the NaH (A) surface are expressed by the classical adsorption isotherms of Langmuir, presuming that the adsorption processes are rapid compared to the surface reactions.

Thus the surface concentrations of B and X1 are given by

$$c_B^* = K_B c_B c^* \quad (7)$$

$$c_{X1}^* = K_{X1} c_{X1} c^* \quad (8)$$

A total balance for the surface sites of NaH is valid. In this case, it can be written as

$$c_B^* + c_{X1}^* + c^* = c_0^*$$

where  $c_0^*$  denotes the total concentrations of the surface sites on NaH. The concentration of vacant sites on the surface is  $c^*$ . The amounts of X2 and X3 on the surface are assumed to be so small that their contribution to the total balance (9) is neglected.

After inserting the relationships (7)-(8) into the site balance equation (9), the concentration of vacant sites ( $c^*$ ) is solved in a trivial way. The information from equations (5)-(6) and (7)-(8) is combined, and the rate equations become

$$R_1' = \frac{k_1'' c_B}{1 + K_B c_B + K_{X1} c_{X1}} \quad (10)$$



$$R_2' = \frac{k_2'' c_{X1}}{1 + K_B c_B + K_{X1} c_{X1}} \quad (11)$$

where  $k_1'' = k_1' K_{BC0}^*$  and  $k_2'' = k_2' K_{X1C0}^*$ . If the adsorption of X1 is small compared to that of B, the term  $K_{X1} c_{X1}$  in the denominators of equations (10) and (11) can be omitted.

According to the stoichiometry, the generation rates can be calculated from

$$r_A = -R_1' - 3R_2' \quad (12)$$

$$r_B = -R_1' \quad (13)$$

$$r_{X1} = R_1' - R_2' \quad (14)$$

$$r_P = R_2' \quad (15)$$

$$r_R = 3R_2' \quad (16)$$

## 2.4 Semibatch reactor model

### 2.4.1 General aspects

For gas-solid and liquid-solid reactions, it is commonly assumed that the overall rate of the process is proportional to the available total surface area ( $A$ ) of the solid material. Consequently, the general mass balance equation for an arbitrary component ( $i$ ) in a perfectly stirred semibatch tank reactor can be generalized to

$$\frac{dn_i}{dt} = r_i A + n'_{oi} \quad (17)$$

where  $n'_{oi}$  denotes the component feed, i.e. added amount of substance per time. In the present case,  $n'_{oi} > 0$  for B, but zero for all the other components, because they exist in batch mode only.

The total surface area of NaH is  $A = n_p A_p$  where  $n_p$  and  $A_p$  denote the number of particles and their individual areas, respectively.

By elementary geometric considerations of ideal geometric particles (slab, long cylinder, sphere) it can be concluded that the active area of a reacting particles at an arbitrary reaction time ( $t$ ) is related to the amount of the solid reagent ( $n$ ) [11],

$$\frac{A}{A_0} = \left( \frac{n_i}{n_{0i}} \right)^{s/(s+1)} \quad (18)$$

where  $A_0$  is the initial area in the beginning of the reaction and  $A$  is the area at an arbitrary time ( $t$ ). The amounts of substance in the beginning ( $n_{0i}$ ) and at an arbitrary time moment ( $t$ ) are the measurable quantities. The shape factor ( $s$ ) is related to the particle geometry, to the ratio of the area ( $A_P$ ) and the volume ( $V_P$ ) of the particle. The relation obeys the general rule [11-12],

$$\frac{A_P}{V_P} = \frac{s+1}{R_P} \quad (19)$$

where  $s=0$  for a slab (flake),  $s=1$  for an infinitely long cylinder and  $s=2$  for a sphere.  $R_P$  is the characteristic dimension of the particle (e.g. radius of the cylinder or sphere). Recently it has been shown by theoretical considerations and verified with experimental data that the treatment of ideal surfaces can be extended to real surfaces with defects, such as cracks and craters [11]. The characteristic feature for this kind of surfaces is that additional surface area is available besides the ideal area, thus  $s>2$  for a non-ideal surface. In the extreme case, a completely porous particle is approached, in which the major part of the area exists inside the particles, in the pores, i.e.  $s \rightarrow \infty$  which implies according to equation (18) that first order kinetics is approached:  $s/(s+1) \rightarrow 1$ . Summa summarum, all non-integer values of the reaction order with respect to the solid component are possible according to equation (18), depending on the particle morphology.

The initial surface area ( $A_0$ ) is related to the total specific surface area ( $\sigma_0$ ) and molar mass ( $M_i$ ) of the particles [11],

$$A_0 = \sigma_0 n_{0i} M_i \quad (20)$$

After inserting this fundamental relation to the expression of  $A/A_0$ , equation (18), we obtain

$$A = n_i^{s/(s+1)} n_{0i}^{1/(s+1)} \sigma_0 M_i \quad (21)$$

In this case,  $i=A$  (NaH), and the general mass balance (17) becomes

$$\frac{dn_i}{dt} = r_i \sigma_0 M_A n_{0A}^{1/(s+1)} n_A^{s/(s+1)} + n'_{0i} \quad (22)$$

for all the components. The factor  $\sigma_0 M_A$  is a scalar constant and can be merged to the rate constants.

The liquid volume in the semibatch reactor is updated according to the formula

$$V_L = V_{0L} + V'_{0L} t \quad (23)$$

where  $V_{0L}$  and  $V'_{0L}$  denote the initial volume and the total volumetric flow rate of the B-solution fed into the reactor. The volumetric flow rate was constant during the experiment.

#### 2.4.2 Dimensionless mass balances – amounts of substance

The mass balance equation (22) can easily be transformed to a dimensionless form by dividing it with the initial amount of the key component,  $y_i = n_i / n_0$ .

The dimensionless mass balance equation becomes

$$\frac{dy_i}{dt} = \alpha r_i y_A^{s/(s+1)} + y'_{0i} \quad (24)$$

where

$$y'_{0i} = n'_{0i} / n_0$$

and  $\alpha = \sigma_0 M_A$ . The mathematical model is a system of ordinary differential equations (ODEs), an initial value problem (IVP) with the initial condition  $y_i = y_i(0)$ .

#### 2.4.3 Dimensionless mass balances – concentrations

Alternatively, the concentrations can be used as the variables in all the calculations. The accumulation term in equation (22) can after differentiation be expressed as

$$\frac{dn_i}{dt} = \frac{d(c_i V_L)}{dt} = V_L \frac{dc_i}{dt} + c_i \frac{dV_L}{dt} \quad (25)$$

where  $dV_L/dt = V'_{0L}$  according to equation (31).

The feed rates of the components are  $n'_{0i} = c_{0i} V'_{0L}$ . Recalling that  $dV_L/dt = V'_{0L}$  and inserting equation (25) to equation (22) gives us the concentration-based mass balance

$$\frac{dc_i}{dt} = V_L^{-1} (r_i \sigma_0 M_A (c_{0A} V_{0L})^{1/(s+1)} (c_A V_L)^{s/(s+1)} + (c_{0i} - c_i) V'_{0L}) \quad (26)$$

After introducing the parameter  $\tau_0 = V_{0L} / V'_{0L}$  the relation between the initial volume and the volume at an arbitrary reaction time ( $t$ ) is obtained,

$$V_L / V_{0L} = 1 + t / \tau_0 \quad (27)$$

A dimensionless concentration vector with the elements ( $x_i$ ) is introduced,  $x_i = c_i / c_0$ . After inserting the dimensionless vector in equation (26), the final form of the dimensionless concentration-based mass balance equation is obtained,

$$\frac{dx_i}{dt} = \frac{x_{0i} - x_i}{\tau_0 (1 + t / \tau_0)} + \alpha \frac{x_A^{s/(s+1)}}{(1 + t / \tau_0)^{1/(s+1)}} r_i \quad (28)$$

which is solved numerically with the initial condition  $x_i = x_i(0)$ .

#### 2.4.4 Rate equations in mass balances

Both modelling approaches, equations (24) and (28) require the calculation of the concentrations which appear in the rate equations (10) and (11). By definition, the concentrations are obtained from the amount of substance and the volume,  $c_i = n_i / V_L$ . The reaction volume in the semibatch reactor is obtained from equation (23). For an experiment with a total feeding time ( $t^*$ ), the end volume ( $V_L^*$ ) is

$$V_L^* = V_{0L} + V'_{0L} t^* \quad (30)$$

Division of with the initial volume gives the ratio

$$\beta = V_L^* / V_{0L} = 1 + V'_{0L} t^* / V_{0L} \quad (31)$$

This ratio ( $\beta$ ) was kept constant in all the experiments, i.e. the same amount of the trimethyl borate solution was added during the course of the experiment. The ratio  $V_{0L} / V'_{0L}$  is denoted by  $\tau_0$ , which is solved from equation (31),

$$\tau_0 = t^* / (\beta - 1) \quad (32)$$

After introducing the dimensionless amounts of substance ( $y_i$ ), according to the definition  $y_i = n_i / n_{0i}$ , all the amounts of substance are expressed as  $n_i = y_i c_0 V_{0L}$ , which is inserted in equation (29) giving the update formula for the concentration,

$$c_i = \frac{y_i c_0}{1 + (\beta - 1)t/t^*} \quad (33)$$

Equation (33) is valid for all the concentrations in the reaction system.

#### 2.4.5 Numerical solution strategy

Both the dimensionless balances (33) (based on dimensionless amounts of substance) and (43) (based on dimensionless concentrations) represent straightforward ordinary differential equation (ODE) systems, initial value problems (IVP), which can be solved numerically with available public and commercial software. For the numerical solution of kinetic problems, algorithms for stiff ODEs are recommended, such as backward difference and semi-implicit Runge-Kutta methods are generally recommended [12], because the values of the kinetic constants in the system can be very different, which contributes to the stiffness of the system. In the present case, the numerical problem was solved with the commercial software gPROMS [13], using the algorithm for stiff ODE-IVPs. In the estimation of the kinetic parameters, the stiff ODE-IVP solver was coupled to an optimization routine, in order to minimize the squared differences between the experimentally observed and by the model predicted product yields (P and X1). In general, the numerical simulations were conducted without any significant problems.

### 3 EXPERIMENTAL EQUIPMENT, PROCEDURES AND KINETIC DATA

#### 3.1 Preparation of NaBH<sub>4</sub> in oil dispersion

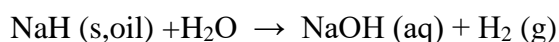
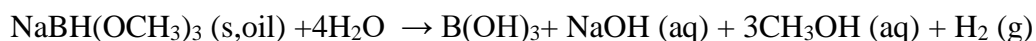
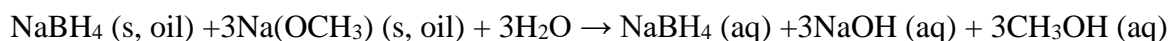
All the experiments were conducted in an isothermal and isobaric stainless-steel reactor, which was operated at 230-270°C under atmospheric pressure. The reactor was equipped with a reflux condenser to prevent the escape of volatile B(OCH<sub>3</sub>)<sub>3</sub> (b.p. 67.4°C at 1 atm). The B(OH)<sub>3</sub> (Merck AG, zur Synthese 98%) needed for the reaction was dissolved in white mineral oil (Marcol) (30-wt-% solution of B(OCH<sub>3</sub>)<sub>3</sub>) and fed into the reactor vessel with a peristaltic pump. The feed rate was constant throughout the experiment. The storage vessel of B(OCH<sub>3</sub>)<sub>3</sub> was placed on a balance to check the feed rate. A dispersion of sodium hydride in mineral oil was prepared in advance from Na (Merck AG) and hydrogen (AGA, 99.99%) and transferred to the reactor,

preheated to the reaction temperature after which the feed of  $B(OCH_3)_3$  was switched on. A blade impeller was used and the stirring speed was 800 rpm (Hans Heidolph Laborrührer) in the systematic kinetic experiments. The feeding times were varied in different experiments in such a way that always the same amount of  $B(OCH_3)_3$  was fed into the reactor. A typical initial mass of the NaH dispersion was 100g and the added mass of  $B(OCH_3)_3$  and mineral oil ( $B(OCH_3)_3$  – mineral oil solution) was 43g. Thus the reaction mass increased by 43% during the experiment. Therefore it was necessary to include also the volume change in the reactor model. After completing the feeding of  $B(OCH_3)_3$ , the experiment was finished and a sample (10g) was withdrawn from the reactor with a vacuum pump and taken to water extraction followed by chemical analysis.

### 3.2 Water extraction

The sample content (unreacted NaH,  $NaBH_4$ ,  $NaOCH_3$ , intermediate by-products, mineral oil) was mixed with water, which lead to the dissolution of  $NaBH_4$  and  $NaOCH_3$  and evolution of  $H_2$  (from unreacted NaH and reaction intermediates). The remains of  $B(OCH_3)_3$  did not contribute to the mass balance in this stage, because  $B(OCH_3)_3$  was either consumed in the reaction or evaporated from the oil phase after completing the experiment. The aqueous extract contained  $NaBH_4$ ,  $CH_3OH$  (from  $NaOCH_3$  and  $NaBH(OCH_3)_3$ ) and  $NaOH$  (from  $NaOCH_3$  and NaH). The extraction was quantitative in 5-10 minutes.

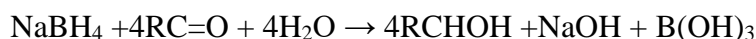
During the water extraction step, the following reactions take place:



The reaction stoichiometry listed above reveals that the first reaction produces the  $CH_3OH$ -to- $NaBH_4$  ratio 3:1 but the second reaction gives additional  $CH_3OH$  because of the decomposition of  $NaBH(OCH_3)_3$ .

### 3.3 Chemical analysis

An analysis method, which would enable to determine both the concentrations of NaBH<sub>4</sub> and CH<sub>3</sub>OH in the aqueous phase was developed. The analysis method was based on the selective reduction capacity of NaBH<sub>4</sub>. By addition of an excess of a ketone, in this case acetone, to the water extract, the double bond of the ketone is reduced by NaBH<sub>4</sub> to a hydroxyl group, according to the stoichiometry (R=carbon chain),



The amount of NaBH<sub>4</sub> in the sample was calculated from the amount of alcohol (2-propanol) formed.

Both products (NaBH<sub>4</sub> and X1=NaBH(OCH<sub>3</sub>)<sub>3</sub>) give three moles of methanol according to the stoichiometry. The amount of NaBH<sub>4</sub> is calculated from  $n_{\text{NaBH}_4} = n_{\text{RCHOH}}/4$ . The excess of methanol reveals the amount of the intermediate by-product:  $n_{\text{NaBH}(\text{OCH}_3)_3} = n_{\text{CH}_3\text{OH}}/3 - n_{\text{NaBH}_4}$ . In case that the methanol amount is exactly 3 times the amount of NaBH<sub>4</sub>, no by-products are formed.

The gas chromatographic (GC) analysis was straightforward. A gas chromatograph (Varian) equipped with a capillary column (stationary phase SE-30) and a flame ionization detector (FID) was used. The carrier gas was helium (3 bar). 1-Propanol was used as the internal standard. All the chemicals (acetone, 1-propanol and 2-propanol, Merck AG ) were of analytical quality. A specified amount of the internal standard, 1-propanol was added to the aqueous sample (0.2-0.3 μL) which was injected to the isothermally operated GC. The injector, column and detector temperatures were 120 °C, 30°C and 150°C, respectively. The response factors of 2-propanol and methanol with respect to 1-propanol were determined from a set of prepared aqueous solutions of these compounds. The response factors of 2-propanol and methanol were  $f_1=1.1514$  and  $f_2=1.7314$ . The components were eluted from the capillary column in the order: methanol, acetone, 2-propanol, 1-propanol. The peak separation in the chromatogram was good and the peak areas were integrated numerically.

## 4 MODELLING RESULTS AND DISCUSSION

The experimental data are displayed in Figure 1. Totally 16 semibatch experiments are reported here; each point of in the yield curve corresponds to one experiment. The yield curves of the final product ( $P = \text{NaBH}_4$ ) show an increasing tendency as a function of the duration of the experiment, whereas the experimentally recorded yields of the intermediate product ( $X1 = \text{NaBH}(\text{OCH}_3)_3$ ) decrease as a function of the duration of the experiment. However, at  $t=0$ , no X1 is present, so the yield of X1 is zero at  $t=0$ . Thus the yield curve of X1 passes a maximum, as indicated by the simulations of the model. The continuous lines in Figure 1 represent the model predictions. The yield of sodium borohydride (P) was improved in prolonged experiments, i.e. longer feeding times of trimethyl borate (B). This is expected, because long reaction times favour the formation of the final product in a consecutive-competitive reaction sequence  $B \rightarrow X1 \rightarrow X2 \rightarrow X3 \rightarrow P$ , where a reagent (here NaH) is added in each step. In fact, NaH, the parallel reagent was always present in excess in the multiphase reaction system, because it was the batch component. This arrangement maximizes the yield of the final product,  $\text{NaBH}_4 (=P)$ . The maximal yield of  $\text{NaBH}_4$  exceeded 90% in the longest experiment at 260°C (Figure 1).

In general, the model describes the experimental data rather well, which is also confirmed by the overall parity plot displayed in Figure 2. No systematic deviations between the experimental data and the model predictions could be detected in the parity plot. The conditions for the parameter estimation and the parameter estimation results are collected in Tables 1 and 2, respectively.

The shape factor  $s=2$ , i.e. spherical particles of NaH was used in the parameter estimation. This is in accordance with visual observations of the NaH dispersion. Preliminary parameter estimation efforts indicated that the kinetic model could be further simplified, because the adsorption effects of trimethyl borate (B) and trimethoxy borohydride (X1) turned out to be minor on the rate equations (10)-(11). A good description of the system was achieved by assuming pseudo-first order kinetics with respect to trimethyl borate and trimethoxy borohydride ( $K_B=0$  and  $K_{X1}=0$  in equations 10-11).



**Table 1. Summary of the parameter estimation procedure**

**Simulation settings:**  $t=0$ :  $y_A=4$ ,  $y_B=0$ ,  $y_{X1}=0$ ,  $y_P=0$ ,  $y_R=0$ ,  $c_0=1$  (arbitrary unit),  $y'_{0B}=1/t^*$ ,  $y'_{0i}=0$  ( $i \neq B$ ),  $t^*$ =total time of the experiment,  $\beta=1.43$ ,  $s=2$

**Functionalities:**

$$k'_j = k'_{j,ref} \exp \left[ -\frac{Ea_j}{R_g} \left( \frac{1}{T} - \frac{1}{T_{ref}} \right) \right], j = 1, 2, T_{ref} = 503.15K$$

$$K_B = K_{B,ref} \exp \left[ -\frac{\Delta H}{R_g} \left( \frac{1}{T} - \frac{1}{T_{ref}} \right) \right], T_{ref} = 503.15K$$

$$k'_j = \sigma_0 M_A k''_j c_0$$

**Table 2 – Parameter estimation results ( $T_{ref}=503.15K=230^\circ C$ ).**

	<b>Value±95%C.I.</b>	<b>Units</b>
$k'_{1,ref}$	0.3014±0.1059	min <sup>-1</sup>
$k'_{2,ref}$	0.1180±0.009	min <sup>-1</sup>
$Ea_1$	104000±50000	J/mol
$Ea_2$	53432±7494	J/mol
$K_{B,ref}$	0	m <sup>3</sup> /mol
$\Delta H$	0	J/mol

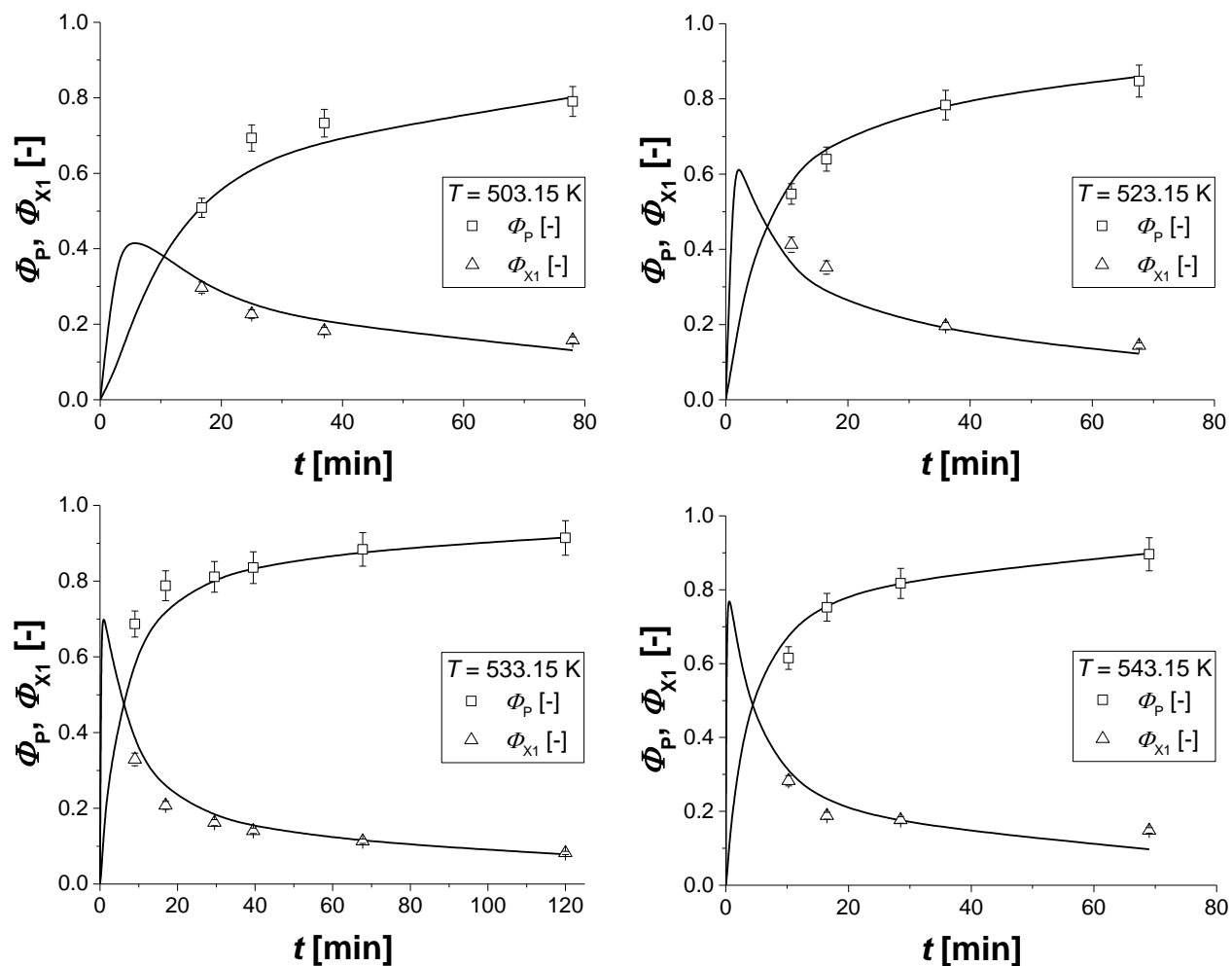


Figure 1. The yields of NaBH<sub>4</sub> (P) and the intermediate product (X1),  $\Phi_P=y_P$ ,  $\Phi_{X1}=y_{X1}$  as a function of the experimental time at four temperatures (230°C, 250°C, 260°C and 270°C). Comparison of experimental data (points) and model predictions (continuous lines).

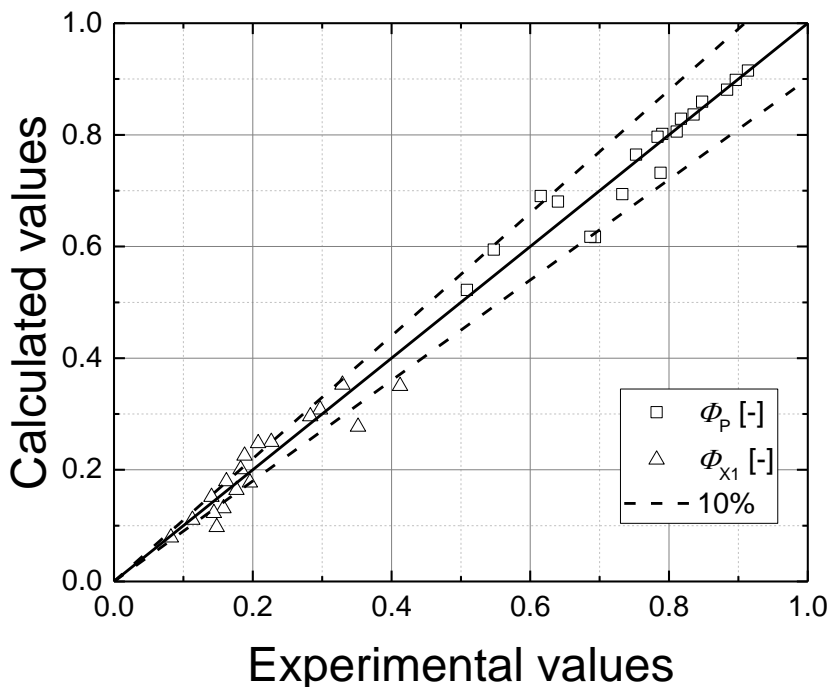


Figure 2. Overall parity plots of the model fit to all the experimental data displayed in Figure 1.

The values of the rate constants at the reference temperature (503.15K=230°C) and the activation energies are reported in Table 2. The activation energy for the formation of NaBH<sub>4</sub> in reaction step 2 was determined to 53.4 kJ/mol. The results reported in Table 1 reveal that the accuracies of the estimated parameters are in most cases reasonably good. The 95% confidence intervals of the parameters are rather small for reaction 2, whereas they are clearly larger for reaction 1, the formation of the reaction intermediate X1. The improvement of the parameter values for reaction 2 value would require experiments at even shorter reaction times, i.e. a more rapid feed of trimethyl borate, which however was not possible for technical and safety reasons – a too rapid addition of trimethyl borate resulted in evaporation of it from the reaction mixture. To check further the effect of the rate parameter of the first reaction, a sensitivity analysis was performed. The value of the rate parameter was changed with 35% from the optimum value reported in Table 2 and the yields of the the final product (P=NaBH<sub>4</sub>) and the intermediate (X1) were simulated at 260°C (533K), which is from a practical viewpoint a very relevant temperature. The simulation results are displayed in Figure 3 which reveals that the model is rather insensitive for this change of the parameter value.

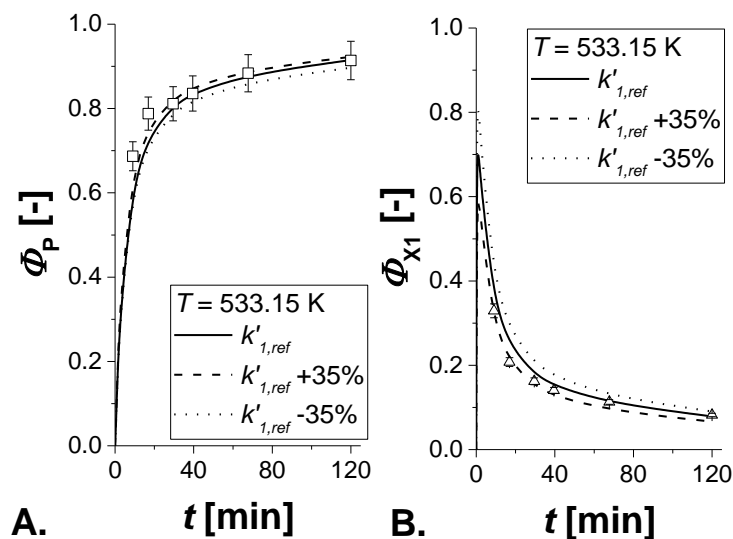


Figure 3. Sensitivity analysis of  $k'_{1,ref}$  parameter in a window of  $\pm 35\%$ . The yields of: A.  $\text{NaBH}_4$  (P); B. the intermediate product (X1), at  $260^\circ\text{C}$ .

A numerical simulation study was carried out by using the estimated kinetic parameters. The dimensionless initial amount of A,  $y_A(t=0)$  was varied between 1 and 4, and the reaction temperatures were  $230^\circ\text{C}$  and  $260^\circ\text{C}$ . The shape factor was  $s=2$  (spherical particles) and the relative amount of trimethyl borate fed to the reactor per time was  $y'_{OB}=1/t^*$ . The results are presented as contour plots in Figures 4 and 5. The figures reveal that long feeding times ( $t^*$ ) and high relative initial amounts of NaH ( $y_A$  at  $t=0$ ) favour the formation of  $\text{NaBH}_4$  (P). A temperature increase leads to higher yields of  $\text{NaBH}_4$  and the maximum of the intermediate product, X1 becomes sharper. This is in accordance with the experimental data displayed in Figure 1: very narrow concentration maxima are predicted at  $260^\circ\text{C}$  and  $270^\circ\text{C}$ .

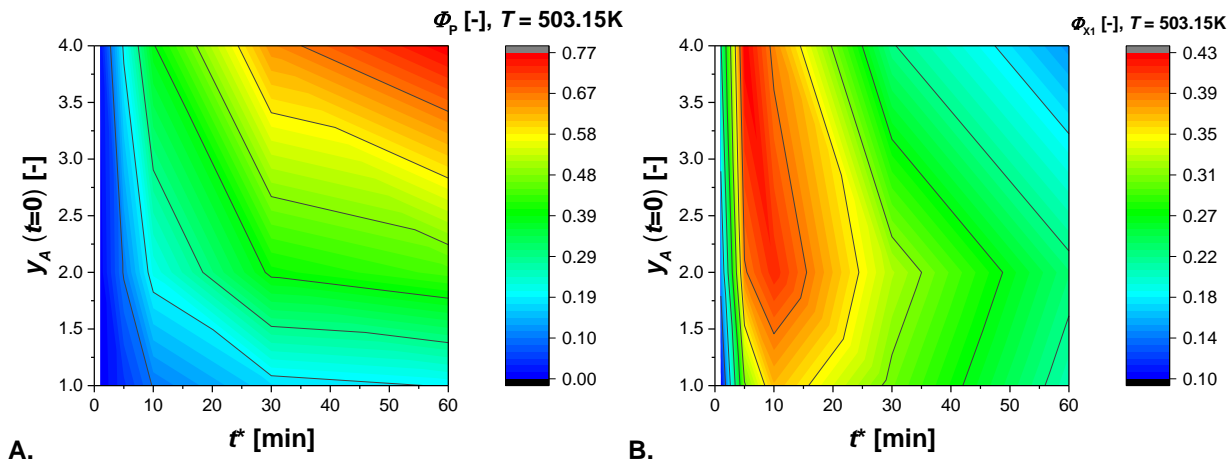


Figure 4. Contour plots for NaBH<sub>4</sub> (P) (A., left) and X1 (B., right) yields as a function of the initial amount of NaH ( $y_A$  at  $t=0$ ) and the experiment stop-time ( $t^*$ ) at 503.15K (230°C).

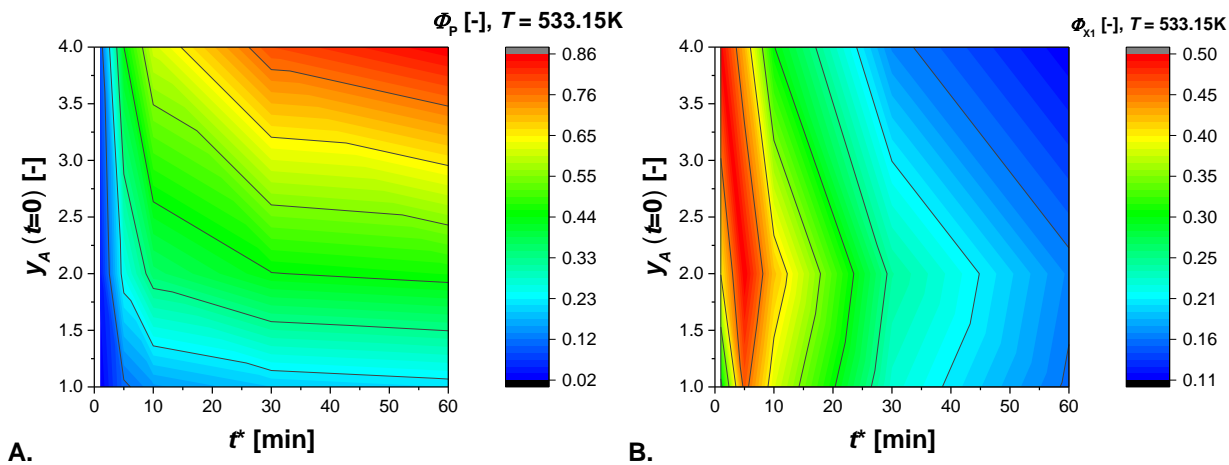


Figure 5. Contour plots for NaBH<sub>4</sub> (P) (A., left) and X1 (B., right) yields as a function of the initial amount of NaH ( $y_A$  at  $t=0$ ) and the experiment stop-time ( $t^*$ ) at 533.15K (260°C).

## 5 CONCLUSIONS

A new mathematical model for the synthesis of sodium borohydride ( $\text{NaBH}_4$ ) from sodium hydride ( $\text{NaH}$ ) and trimethyl borate ( $\text{B}(\text{OCH}_3)_3$ ) in mineral oil was introduced. The model is based on the hypothesis of the adsorption of trimethyl borate on the surfaces of dispersed sodium hydride particles in mineral oil. A plausible molecular reaction mechanism was proposed for the stepwise addition of hydrogen from  $\text{NaH}$  to trimethyl borate. This hypothesis gave a set of rate equations for the formation of  $\text{NaBH}_4$  and the intermediate by-products. The complete stoichiometric model was simplified to comprise only one by-product ( $\text{X1}=\text{NaBH}(\text{OCH}_3)_3$ ), which has been confirmed experimentally. The simplified kinetic model was verified with experimental data obtained from a laboratory-scale semibatch reactor. The model reproduced the experimental data well indicating that the physical and chemical hypotheses of the model are reasonable. The accuracy of the model was better for the prediction of the concentration of the final product ( $\text{P}=\text{NaBH}_4$ ), but the model was less accurate for the prediction of the reaction intermediate ( $\text{X1}$ ). Taking into account these aspects, the results can be used for reactor analysis and process optimization.

## NOTATION

$A$	total surface area, $\text{m}^2$
$A_0$	initial total surface area, $\text{m}^2$
$A_P$	surface area of a particle, $\text{m}^2$
$a_j$	merged parameter for reaction step $j$
$\mathbf{a}'$	vector for chemical components
$c_i$	concentration of component $i$ , $\text{mol}/\text{m}^3$
$\mathbf{c}$	concentration vector, $\text{mol}/\text{m}^3$
$c^*$	concentration on the sodium hydride surface, $\text{mol}/\text{m}^2$
$c_0$	reference concentration, $\text{mol}/\text{m}^3$
$d_P$	particle diameter ( $=2R_P$ ), $\text{m}$
$E_a$	activation energy, $\text{J}/\text{mol}$
$f$	response factor in gas-chromatographic analysis

$\Delta H$	enthalpy, J/mol
$K$	adsorption equilibrium constant, m <sup>3</sup> /mol
$k$	reaction rate constant
$k', k''$	merged rate constants
$M$	molar mass, kg/mol
$N, N'$	stoichiometric matrices
$n_i$	amount of substance, mol
$\mathbf{n}$	amount of substance vector, mol
$\mathbf{n}'_0$	inlet molar flow vector, mol/s
$n_P$	number of particles in the liquid phase
$R_j, R'_j$	rates of reaction step $j$ , mol/(m <sup>2</sup> ·s)
$\mathbf{R}'$	reaction rate vectors, mol/(m <sup>2</sup> ·s)
$R_P$	characteristic dimension of the particle, particle radius, m
$R_g$	gas constant, 8.3143 J/(Kmol)
$\mathbf{r}, \mathbf{r}'$	generation rate vectors, mol/(m <sup>2</sup> ·s)
$s$	shape factor, -
$T$	temperature, K (or °C)
$t$	time, s
$t^*$	total feeding time of B(OCH <sub>3</sub> ) <sub>3</sub> , time of the semibatch experiment, s
$V_L$	liquid volume, m <sup>3</sup>
$V_P$	volume of a particle, m <sup>3</sup>
$V'_0$	volumetric flow rate of the feed, m <sup>3</sup> /s
$X$	conversion of sodium hydride
$x_i$	dimensionless concentration of component $i$ , -
$\mathbf{x}$	dimensionless concentration vector
$y$	dimensionless amount of substance $i$ , -
$\mathbf{y}$	dimensionless amount of substance vector, -
<i>Greek letters</i>	
$\alpha$	parameter, $\alpha = \sigma_0 M_A$ , m <sup>2</sup> /mol
$\sigma_0$	specific surface area of the particle, m <sup>2</sup> /kg
$\beta$	final-to-initial volume ratio of the reactor content, -
$\nu$	stoichiometric coefficient, -

$\rho$	density, kg/m <sup>3</sup>
$\tau_0$	time constant, $\tau_0 = V_{0L}/V'_{0L}$ , s
$\Phi$	yield, -



*Subscripts and superscripts*

i	component
j	reaction step
L	liquid
P	particle
ref	reference
T	transpose of a matrix or vector
*	surface site
0	initial state or inlet condition

*Abbreviations*

A	NaH
B	B(OCH <sub>3</sub> ) <sub>3</sub>
P	NaBH <sub>4</sub>
R	NaOCH <sub>3</sub>
X1	NaBH(OCH <sub>3</sub> ) <sub>3</sub>
X2	NaBH <sub>2</sub> (OCH <sub>3</sub> ) <sub>2</sub>
X3	NaBH <sub>3</sub> (OCH <sub>3</sub> )

**ACKNOWLEDGEMENT**

This work is a part of activities at the Johan Gadolin Process Chemistry Centre (PCC), a centre of excellence in scientific research financed by Åbo Akademi University. Financial support from Academy of Finland, Academy Professor grant (319002) to T. Salmi is gratefully acknowledged. The authors are grateful to Professor Dr. L.-E. Lindfors, Professor Dr E. Y. O. Paatero and Mr B. Sjöberg for inspiring discussions and constructive proposals during the experimental work. The article is dedicated to the memory of Professor, PhD (MIT) Leif Hummelstedt.

## REFERENCES

- [1] Kirk-Othmer Encyclopedia of Chemical Technology, 4<sup>th</sup> Ed., Vol 13, 606-629, Wiley (1995)
- [2] Ullmann's Encyclopedia of Industrial Chemistry, 6<sup>th</sup> Ed., Vol 16, 721-7226, Wiley-VCH Weinheim (2003)
- [3] Schlesinger, H.J., Brown, H.C., Abraham, B., Bond, A.C., Davidson, N., Finholt, A.E., Gilbreath, J.R., Hoekstra, H., Horvitz, L., Hyde, E.K., Katz, J.J., Knight, J., Lad, R.A., Mayfield, D.L., Rapp, L., Ritter, D.M., Schwartz, A.M., Sheft, I., Tuck, L.D., Walker A.O., New Developments in the Chemistry of Diborane and the Borohydrides. I. General Summary, Journal of American Chemical Society 75, 186-190 (1953)
- [4] Schlesinger, H.J., Brown, H.C., Sheft, I., Ritter, D.M., Addition Compounds of Alkali Metal Hydrides. Sodium Trimethoxyborohydride and Related Compounds, Journal of American Chemical Society 75, 192-195 (1953)
- [5] Schlesinger, H.J., Brown, H.C., Finholt, A.E., The Preparation of Sodium Borohydride by the High Temperature Reaction of Sodium Hydride with Borate Esters, Journal of American Chemical Society 75, 205-209 (1953)
- [6] Kreevoy, M.M., Jacobson, R.W., The Rate of Decomposition of NaBH<sub>4</sub> in Basic Aqueous Solutions, Ventron Alembic 15, 2-3 (1979)
- [7] Schubert, F., Lang, K., Neue Wege zur Herstellung von Natriumboratan und dessen Verwendung, Angewandte Chemie 72, 994-1000 (1960)
- [8] Pecak, V., Vit, J., Maschine und Werkzeug 68, 36 (1967)
- [9] Wu, Y., Kelly, M.T., Ortega, J., Review of Chemical Processes for the Synthesis of Sodium Borohydride, Millenium Cell Inc, Under DOE Cooperativ Agreement DE-FC36-04GO14008, , August 2004
- [10] Li, Z.P., Morigazaki, N., Liu, B.H., Suda, S., Preparation of sodium borodhydride by the reaction of MgH<sub>2</sub> with dehydrated bórax through ball milling at room temperatura, Journal of Alloys and Compounds 349 (2003) 232-236
- [11] Salmi, T., Grénman, H., Wärnå, J., Murzin, D. Yu., Revisiting shrinking particle and product layer for fluid-solid reactions – from ideal surfaces to real surfaces, Chemical Engineering and Processing: Process Intensification 50, 1076-1094 (2011)
- [12] Salmi, T., Mikkola, J.-P., Wärnå, J., Chemical Reaction Engineering and Reactor Technology, CRC Press Taylor & Francis Group Boca Raton Fl., p. 311 (2011)
- [13] gPROMS, Process Systems Enterprise (2018)

## SUPPLEMENTARY MATERIAL: EXPERIMENTAL DATA

Time (t)/ xx/min.yy/s, e.g. 16.45 = 16 min 45 s

Rotation speed of the stirrer  $r = 800 \text{ min}^{-1}$

230°C

t	$\Phi_P$	$\Phi_{X1}$
0	0	0
16.45	50.88	29.71
25	69.33	22.67
37	73.28	18.25
78	79.04	15.79

250°C

t	$\Phi_P$	$\Phi_{X1}$
0	0	0
10.45	54.75	41.25
16.30	63.99	35.19
36	78.36	19.59
67.40	84.77	14.41

260°C

t	$\Phi_P$	$\Phi_{X1}$
0	0	0
9	68.68	32.92
16.55	78.79	20.77
29.30	81.12	16.20
39.30	83.56	14.05
67.45	88.37	11.31
120	91.39	8.21

270°C

t	$\Phi_P$	$\Phi_{X1}$
10.15	61.51	28.29
16.30	75.25	18.81
28.30	81.72	17.65
69.00	89.63	14.82